MITSUBISHI ELECTRIC RESEARCH LABORATORIES
http://www.merl.com

Online Parameter Identification for State of Power Prediction of Lithiumion Batteries in Electric Vehicles Using Extremum Seeking

Wei, C.; Benosman, M.; Kim, T.

TR2019-085 September 05, 2019

Abstract

Accurate state-of-power (SOP) estimation is critical for building battery systems with optimized performance and longer life in electric vehicles and hybrid electric vehicles. This paper proposes a novel parameter identification method and its implementation on SOP prediction for lithium-ion batteries. The extremum seeking algorithm is developed for identifying the parameters of batteries on the basis of an electrical circuit model incorporating hysteresis effect. A rigorous convergence proof of the estimation algorithm is provided. In addition, based on the electrical circuit model with the identified parameters, a battery SOP prediction algorithm is derived, which considers both the voltage and current limitations of the battery. Simulation results for lithium-ion batteries based on real test data from urban dynamometer driving schedule (UDDS) are provided to validate the proposed parameter identification and SOP prediction methods. The proposed method is suitable for real operation of embedded battery management system due to its low complexity and numerical stability.

International Journal of Control, Automation and Systems

International Journal of Control, Automation and Systems 17(X) (2019) 1-11
http://dx.doi.org/10.1007/s12555-018-0506-y
ISSN:1598-6446 eISSN:2005-4092
http://www.springer.com/12555

Online Parameter Identification for State of Power Prediction of Lithium-ion Batteries in Electric Vehicles Using Extremum Seeking

Chun Wei*, Mouhacine Benosman, and Taesic Kim

Abstract: Accurate state-of-power (SOP) estimation is critical for building battery systems with optimized performance and longer life in electric vehicles and hybrid electric vehicles. This paper proposes a novel parameter identification method and its implementation on SOP prediction for lithium-ion batteries. The extremum seeking algorithm is developed for identifying the parameters of batteries on the basis of an electrical circuit model incorporating hysteresis effect. A rigorous convergence proof of the estimation algorithm is provided. In addition, based on the electrical circuit model with the identified parameters, a battery SOP prediction algorithm is derived, which considers both the voltage and current limitations of the battery. Simulation results for lithium-ion batteries based on real test data from urban dynamometer driving schedule (UDDS) are provided to validate the proposed parameter identification and SOP prediction methods. The proposed method is suitable for real operation of embedded battery management system due to its low complexity and numerical stability.

Keywords: Battery management system, extremum seeking, lithium-ion battery, parameter identification, state of power.

1. INTRODUCTION

Electric vehicle (EV) and hybrid electric vehicle (HEV) are two promising solutions to relief the energy crisis and environmental issues raised by the oil-dependent vehicles [1]. The core component of the EV and HEV is the battery system. Lithium-ion batteries have been widely used in EVs and HEVs due to their high energy and power densities and long cycle life [2]. However, effective battery management system (BMS) is still a remarkable challenge and necessity to guarantee the reliable and safe battery operations [3]. The critical function of the BMS is to estimate the state-of-charge (SOC), state-of-health (SOH), and state-of-power (SOP) of the battery system in real-time [4]. Due to the absence of sensors for direct measurements of these quantities, battery models are used to estimate these states based on model-based estimation methods. To improve the SOC, SOH, and SOP estimation accuracy of lithium-ion batteries, the parameters of the battery model should be identified effectively.

Various algorithms have been proposed for the parameter estimation or identification of lithium-ion batteries. Kalman filter (KF)-based methods and linear least square regression-based methods are two main types of real-time battery parameter identification methods. Various types of KF have been proposed [5–11], such as linear KF, extended KF (EKF), dual extended KF, to estimate the parameters and the states of the battery model simultaneously. Although accurate solutions can be obtained by using KF-based methods, they cause high computational complexity and may be difficult to implement in real-time embedded systems. Compared to the KF-based methods, the least squares methods are more computationally competitive without losing much accuracy. Various least square-based methods have been proposed, such as recursive least square [12,13], and moving window least square [14], to perform online estimation of battery parameters. A prediction-error minimization algorithm was used to identify battery model parameters for SOC estimation in [15]. Sliding-mode observer and neural networks were used in [16] for SOC estimation of a lithium-polymer battery in electric vehicle. In [17], a robust H_∞ filter was proposed for the first time to estimate the SOC of the lithium-ion battery system with time-varying parameter for hybrid electric vehicles. Although these methods presented accepted performance, they required high computational re-

Manuscript received July 17, 2018; revised December 8, 2018 and March 10, 2019; accepted June 13, 2019. Recommended by Associate Editor Yongping Pan under the direction of Editor Young IL Lee. This work is supported by the National Natural Science Foundation of China under Grants No.51807179 and No.51777193, and The Key Research and Development Program of Zhejiang Provience under Grants No.2019C01149.

Chun Wei is with the College of Information Engineering, Zhejiang University of Technology, Hangzhou, Zhejiang 310023, China (e-mail: chunwei18@zjut.edu.cn). Mouhacine Benosman is with Mitsubishi Electric Research Laboratories, Cambridge, MA 02139, USA (e-mail: benosman@merl.com). Taesic Kim is with the Department of Electrical Engineering and Computer Science, Texas AM University-Kingsville, Kingsville, TX 78363, USA (e-mail: taesic.kim@tamuk.edu).
* Corresponding author.

sources and sometimes got stuck in local optima due to a large number of parameters and a very large searching space [18].

The estimation of the peak power capability of the battery is essential to determine the maximum available power for acceleration and regenerating braking of the EV and HEV, thus avoiding over-charging or over-discharging the battery. SOP is the parameter to describe the maximum charging and discharging capabilities of the battery [19]. Accurate SOP estimation can guarantee optimum performance and longer life of the battery. A dynamic electrochemical polarization model is proposed in [20], and the battery SOP for the next sampling time is accurately estimated based on this model. An adaptive extended KF is proposed to estimate the SOC and SOP simultaneously in [21], which realizes a long-term SOP estimation. First-order extrapolation and multistep model predictive iterative method were used in [22] to improve voltage-limit-based power output accuracy in larger time intervals and a genetic algorithm was proposed in [23] to deal with the long time-scale estimation for power management application. However, only the voltage limitation is considered in the above researches when calculating the peak power capability, the battery current limitation is ignored.

This paper proposes a novel parameter identification method and its implementation on SOP prediction for lithium-ion batteries in EVs using extremum seeking (ES) theory, which is a model-free adaptive optimization method and has the advantages of both rigorously provable convergence and simple implementation [24–27]. The estimated battery parameters can then be used for online SOC, SOH, and SOP estimation for lithium-ion batteries. In this paper, based on the electrical circuit model with the identified parameters, a battery SOP prediction algorithm is derived, which considers both the voltage and current limitations of the battery. Simulation results for lithium-ion batteries based on real test data from urban dynamometer driving schedule (UDDS) are provided to validate the proposed parameter identification and SOP prediction methods. The proposed method is suitable for real operation of embedded battery management system due to its low complexity and numerical stability.

2. THE BATTERY MODEL

The battery model should be carefully chosen to ensure a precise estimation of states and parameters. For real-time application in embedded systems, a balance between the accuracy and complexity of the battery model should be made. Electrical circuit battery models are the most suitable for embedded applications due to their low complexity and the ability of characterizing the current-voltage (I-V) dynamics of battery cells [28]. The voltage hysteresis effect between the charging and discharging widely exists in Li-ion batteries, especially for the $LiFePO_4$-type. It is demonstrated that the first-order resistor-capacitor (RC) model with one-state hysteresis seems to be the best choice for $LiFePO_4$ cells [29]. Therefore, the first-order RC model with a hysteresis, as shown in Fig. 1, is used in this paper to provide a good balance between model accuracy and complexity.

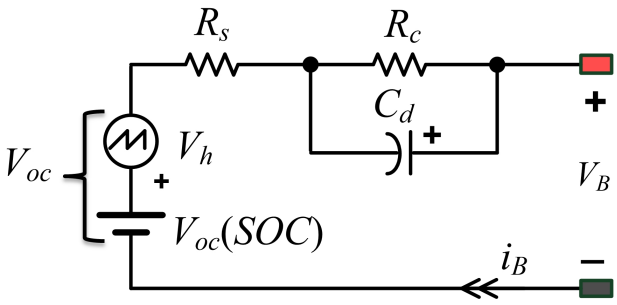

Fig. 1. The first-order RC model with hysteresis.

As shown in Fig. 1, the open-circuit voltage (OCV) V_{oc} includes two parts. The first part, $V_{oc}(SOC)$, represents the equilibrium OCV as a function of the SOC. The second part V_h is the hysteresis voltage to capture the hysteresis behavior of the OCV curves. The RC circuit models the I-V characteristics and the transient response of the battery cell. The series resistance, R_s, is used to describe the charge/discharge energy loss in the cell; the charge transfer resistance, R_c, and double layer capacitance, C_d, are used to characterize the charge transfer and short-term diffusion voltage, V_d, of the cell; V_B represents the terminal voltage of the cell.

The following voltage hysteresis model is used [5]:

$$\frac{\partial V_h}{\partial t} = -\rho\left(\eta i_B - vS_D\right)\left[V_{hmax} + sign(i_B)V_h\right], \tag{1}$$

where ρ is the hysteresis parameter representing the convergence rate, η is the Coulomb efficiency (assuming η=1), i_B is the instantaneous current applied to the battery, v is the self-discharge multiplier for hysteresis expression, S_D is the self-discharge rate, and V_{hmax} is the maximum hysteresis voltage. The model (1) describes the dependency of the hysteresis voltage V_h on the current, self-discharge, and hysteresis boundaries. The parameter ρ is chosen to minimize the voltage error between the V_{oc}-SOC curves from simulation and experiments, respectively.

The self-discharge effect is ignored in order to reduce the complexity of the battery model, so a simplified continuous-time state space model can be obtained as follows:

$$\frac{\partial V_h}{\partial t} = -\rho i_B sign(i_B)V_h - \rho V_{hmax} i_B. \tag{2}$$

A discrete-time version of (2) assuming that i_B and V_{hmax} are constant over the sample period can be written

as follows:

$$V_h(k+1) = \exp(-\rho|i_B|T_s)V_h(k) + (\exp(-\rho|i_B|T_s)-1)sign(i_B)V_{hmax}, \quad (3)$$

where T_s is the sampling period and k is the time index.

Therefore, combined with the electrical circuit part, a discrete-time battery model, including the electrical circuit model and the hysteresis model, can be written as follows:

$$\begin{aligned} X(k+1) &= \begin{bmatrix} 1 & 0 & 0 \\ 0 & \gamma & 0 \\ 0 & 0 & H \end{bmatrix} X(k) \\ &\quad + \begin{bmatrix} -\frac{\eta T_s}{C_{max}} & 0 \\ R_c(1-\gamma) & 0 \\ 0 & (H-1)sign(i_B) \end{bmatrix} \begin{bmatrix} i_B(k) \\ V_{hmax} \end{bmatrix}, \\ y(k) &= V_B(k) = V_{oc}(SOC(k)) - V_d(k) - R_s i_B(k) + V_h(k), \\ V_{oc}(SOC) &= A_0\exp(-a_1 SOC) + A_2 + A_3 SOC \\ &\quad - A_4 SOC^2 + A_5 SOC^3, \end{aligned} \quad (4)$$

where $X(k+1) = [\ SOC(k+1) \quad V_d(k+1) \quad V_h(k+1)\ ]^T$ is the state, $y(k)$is the measured output, C_{max} denotes the maximum capacity of the battery, $\gamma = \exp(\frac{-T_s}{\tau})$ with $\tau = R_c C_d$, $H(i_B) = \exp(-\rho|i_B|T_s)$, and A_j for $0 \le j \le 5$ are the coefficients used to parameterize the V_{oc}-SOC curve. Coefficients A_j for $0 \le j \le 5$ can be extracted by pulsed current tests or constant charge and discharge current test using a small current to minimally excite transient response of the battery cell [30].

3. ES-BASED PARAMETER IDENTIFICATION OF LITHIUM-ION BATTERY

3.1. Basic of ES

The basic scheme for a single gradient-based ES algorithm is shown in Fig. 2. The algorithm injects a sinusoidal perturbation $a\sin(\omega t - \frac{\pi}{2})$ into the system, resulting in an output of the cost function $Q(\theta)$. This output $Q(\theta)$ is subsequently multiplied by $a\sin(\omega t + \frac{\pi}{2})$. The resulting signal after multiplying a gain l, $\dot{\xi}$, is an estimate of the gradient of the cost function with respect to θ. The gradient estimate is then passed through an integrator $\frac{1}{s}$ and added to the modulation signal $asin(\omega t - \frac{\pi}{2})$. The corresponding equations for the basic multi-parameter ES algorithm are:

$$\dot{\xi}_i = a_i l \sin(\omega_i t + \pi/2)Q(\theta), \quad (5)$$

$$\theta_i = \xi_i + a_i \sin(\omega_i t - \pi/2), \quad (6)$$

where a_i is a gain, ω_i is frequency, i is an integer, and $\omega_i > \omega^*$, with ω^* large enough to ensure the convergence. If the parameters a_i, ω_i, and l are properly selected, the cost function output $Q(\theta)$ will converge to a neighborhood of the optimal cost function value $Q(\theta^*)$.

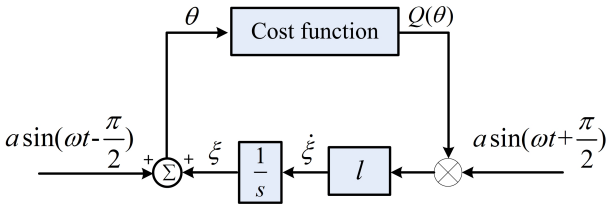

Fig. 2. Block diagram of the basic gradient-based extremum seeking algorithm.

In order to implement the ES algorithm in the real-time embedded system, a discrete version of the ES algorithm is required. The discrete version of the ES algorithm is given:

$$\xi_i(k+1) = \xi_i(k) + a_i l \Delta T \sin(\omega_i k + \pi/2)Q(\theta(k)), \quad (7)$$

$$\theta_i(k+1) = \xi_i(k+1) + a_i \sin(\omega_i k - \pi/2), \quad (8)$$

where k is the time step and ΔT is the sampling time.

3.2. ES for parameter identification

The multi-parameter ES algorithm is used to identify the parameters of the battery model, i.e., R_s, R_c, C_d, and C_{max} in (4). The block diagram of ES-based parameter identification method for lithium-ion battery is shown in Fig. 3. At each time step, a battery terminal voltage V_B can be measured under a specific operating current i_B. The measured V_B is compared with the estimated battery terminal voltage $\hat{V}_B$, which is obtained from the battery model based on the measured current i_B using the estimated battery model parameters. The error of V_B and $\hat{V}_B$ is used to generate a cost function, which represents the convergence of the battery parameters. The battery parameters will then be updated by the ES algorithm and used to generate a new $\hat{V}_B$ in the next time step. The parameter updating process will proceed until the cost function reaches to a small criterion or the algorithm reaches the maximum iteration number.

Using the estimated parameters, the battery model (4)

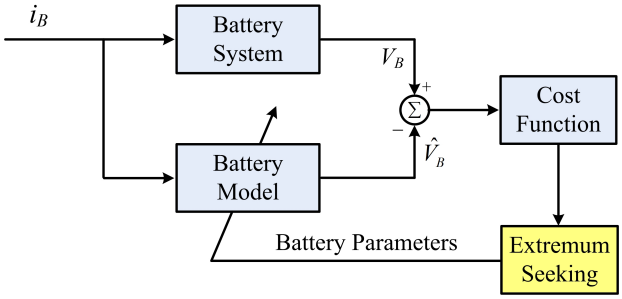

Fig. 3. Extremum seeking-based parameter identification method for lithium-ion battery.

can be written as

$$\begin{aligned}
S\hat{O}C(k+1) &= S\hat{O}C(k) - \frac{\eta T_s}{\hat{C}_{max}} i_B(k),\\
\hat{V}_d(k+1) &= \gamma(k)\hat{V}_d(k) + \hat{R}_c(k)(1-\gamma) i_B(k),\\
\hat{V}_h(k+1) &= H\hat{V}_h(k) + (H-1) sign(i_B(k)) V_{hmax},\\
\hat{V}_B(k) &= V_{oc}(SOC(k)) - \hat{V}_d(k) - \hat{R}_s(k) i_B(k) + \hat{V}_h(k),
\end{aligned} \tag{9}$$

where $\gamma(k) = \exp(\frac{-T_s}{\tau(k)})$, and $\tau(k) = \hat{R}_c(k)\hat{C}_d(k)$.

The following cost function is defined for each iteration:

$$Q(\theta(k)) = K_p \int_{t_0}^{t_f} [V_B(t) - \hat{V}_B(t)]^2 dt, \tag{10}$$

where $[t_0, t_f]$ is the time interval over which the cost function is estimated, and K_p is a gain, and

$$\theta(k) = [\hat{R}_s(k), \hat{R}_c(k), \hat{C}_d(k), \hat{C}_{max}(k)]^T.$$

The battery model parameters are updated in the following algorithm:

$$\begin{aligned}
\hat{R}_s(k+1) &= R_{s,nominal} + \delta\hat{R}_s(k),\\
\hat{R}_c(k+1) &= R_{c,nominal} + \delta\hat{R}_c(k),\\
\hat{C}_d(k+1) &= C_{d,nominal} + \delta\hat{C}_d(k),\\
\hat{C}_{max}(k+1) &= C_{max,nominal} + \delta\hat{C}_{max}(k),
\end{aligned} \tag{11}$$

where $R_{s,nominal}$, $R_{c,nominal}$, $C_{d,nominal}$, and $C_{max,nominal}$ are the nominal initial values of the battery model parameters; $\delta\hat{R}_s(k)$, $\delta\hat{R}_c(k)$, $\delta\hat{C}_d(k)$, and $\delta\hat{C}_{max}(k)$ are the variations of the identified battery model parameters, which are calculated by (12). Following (7) and (8), the variations of the identified battery model parameters are given by

$$\begin{aligned}
\xi_1(k+1) &= \xi_1(k) + a_1 l\Delta T \sin(\omega_1 k + \pi/2) Q(\theta(k)),\\
\hat{\delta}\hat{R}_s(k) &= \xi_1(k+1) + a_1 \sin(\omega_1 k - \pi/2),\\
\delta\hat{R}_s(k) &= \hat{\delta}\hat{R}_s(I-1)T, (I-1)T \le k\Delta T \le IT,\\
\xi_2(k+1) &= \xi_2(k) + a_2 l\Delta T \sin(\omega_2 k + \pi/2) Q(\theta(k)),\\
\hat{\delta}\hat{R}_c(k) &= \xi_2(k+1) + a_2 \sin(\omega_2 k - \pi/2),\\
\delta\hat{R}_c(k) &= \hat{\delta}\hat{R}_c(I-1)T, (I-1)T \le k\Delta T \le IT,\\
\xi_3(k+1) &= \xi_3(k) + a_3 l\Delta T \sin(\omega_3 k + \pi/2) Q(\theta(k)),\\
\hat{\delta}\hat{C}_d(k) &= \xi_3(k+1) + a_3 \sin(\omega_3 k - \pi/2),\\
\delta\hat{C}_d(k) &= \hat{\delta}\hat{C}_d(I-1)T, (I-1)T \le k\Delta T \le IT,\\
\xi_4(k+1) &= \xi_4(k) + a_4 l\Delta T \sin(\omega_4 k + \pi/2) Q(\theta(k)),\\
\hat{\delta}\hat{C}_{max}(k) &= \xi_4(k+1) + a_4 \sin(\omega_4 k - \pi/2),\\
\delta\hat{C}_{max}(k) &= \hat{\delta}\hat{C}_{max}(I-1)T, (I-1)T \le k\Delta T \le IT,
\end{aligned} \tag{12}$$

where a_1, a_2, a_3, and a_4 are positive, $\omega_p + \omega_q \neq \omega_r$, $p,q,r \in \{1,2,3,4\}$, for $p \neq q \neq r$, $I = 1,2,\cdots$ are the learning iterations indexes. When the ES algorithm is used, the gain l in (12) can also be various relating to different parameters.

Remark 1: One can notice that we have introduced extra variables $\hat{\delta}\hat{R}_s$, $\hat{\delta}\hat{R}_c$, $\hat{\delta}\hat{C}_d$, $\hat{\delta}\hat{C}_{max}$, which are needed to differentiate between the two time scales; ΔT the sampling time scale, and T the learning iteration time scale, where $\Delta T < T$. In other words, during each learning iteration IT we keep track of the parameters estimation computed at a faster samplign time ΔT, but we only keep as a final estimate for the learning iteration IT, the values of $\hat{\delta}\hat{R}_s$, $\hat{\delta}\hat{R}_c$, $\hat{\delta}\hat{C}_d$, $\hat{\delta}\hat{C}_{max}$ at $(I-1)T$.

Indeed, the algorithm (10), (11), and (12) are implemented as follows:

1) Initialize all variables ξ_i, $i = 1,\cdots,4$, and $\hat{\delta}\hat{R}_s$, $\hat{\delta}\hat{R}_c$, $\hat{\delta}\hat{C}_d$, $\hat{\delta}\hat{C}_{max}$ to zero.

2) For $I = 1,\cdots,N$, (N is the number of learning iterations):

(i) Integrate forward the equations of ξ_i, $i = 1,\cdots,4$, and the equations of $\hat{\delta}\hat{R}_s$, $\hat{\delta}\hat{R}_c$, $\hat{\delta}\hat{C}_d$, $\hat{\delta}\hat{C}_{max}$, for all k, s.t., $(I-1)T \le k\Delta T \le IT$.

(ii) At the end of each learning interval $[(I-1)T, IT]$, i.e., when $k\Delta T = IT$, update the values of the parameters $\delta\hat{R}_s$, $\delta\hat{R}_c$, $\delta\hat{C}_d$, $\delta\hat{C}_{max}$ as the last values attained by $\hat{\delta}\hat{R}_s$, $\hat{\delta}\hat{R}_c$, $\hat{\delta}\hat{C}_d$, $\hat{\delta}\hat{C}_{max}$. Keep these values of $\delta\hat{R}_s$, $\delta\hat{R}_c$, $\delta\hat{C}_d$, $\delta\hat{C}_{max}$ constants for the next learning iteration, and loop back to 2.(1).

3.3. Convergence analysis

To be able to write a formal convergence analysis, we first need to introduce the following assumptions.

Assumption 1: The ES cost function Q has a local minimum at the true parameters $\theta^* = [R_s, R_c, C_d, C_{max}]^T$.

Assumption 2: The original parameters estimates vector, i.e., the nominal parameters value, is close enough to the actual parameters vector.

Assumption 3: The cost function is analytic and its variation with respect to the uncertain variables is bounded in the neighborhood of θ^*.

We summarize the convergence of the ES estimation algorithm in the following Lemma.

Lemma 1: The ES estimation algorithm (10), (11), and (12), under assumptions 1, 2, 3, where the dither frequencies ω_p, $p \in \{1,2,3,4\}$ are such that $\omega_p > \omega^*$, with ω^* large enough, asymptotically converges to the true values, with the estimation upper-bound

$$\|\theta(\Delta T k) - \theta^*\| \le \frac{\varepsilon_1}{\omega_0} + \sqrt{\sum_{i=1}^{i=4} a_i^2},$$

where $\varepsilon_1 > 0$, and $\omega_0 = max\{\omega_1,\cdots,\omega_4\}$.

Proof: First, based on Assumptions 1, 2, and 3, the ES nonlinear dynamics in (12) can be approximated by

a linear averaged dynamic (using averaging approximation over time ([27], Definition 1)). Furthermore, $\exists\theta_1, \omega^*$, such that for all $\omega_0 = max\{\omega_1, \omega_2, \omega_3, \omega_4\} > \omega^*$, the solution of the averaged model $\theta_{aver}(t)$ is locally close to the solution of the original ES dynamics and satisfies (e.g., refer to [25], [26], [27], [32])

$$\|\theta(t) - d(t) - \theta_{aver}(t)\| \leq \frac{\varepsilon_1}{\omega_0}, \ \ \varepsilon_1 > 0, \ \ \forall t \geq 0$$

with $d(t) = [a_1 \sin(\omega_1 t + \pi/2), \cdots, a_4 \sin(\omega_4 t + \pi/2)]^T$. Next, using the analytic property of the cost function and the proper choice of the dither frequencies, such that $\omega_p + \omega_q \neq \omega_r, p, q, r \in \{1,2,3,4\}$, for $p \neq q \neq r$, allows us to prove that (e.g., see [27], [32])

$$\lim_{t\to\infty} \theta_{aver}(t) = \theta^*.$$

This together with the previous inequality leads to

$$\begin{aligned}
&\|\theta(t) - \theta^*\| - \|d(t)\| \leq \|\theta(t) - \theta^* - d(t)\| \leq \frac{\varepsilon_1}{\omega_0}, \\
&\quad \varepsilon_1 > 0, \ \ t \to \infty, \\
&\|\theta(t) - \theta^*\| \leq \frac{\varepsilon_1}{\omega_0} + \|d(t)\|, \ \ \varepsilon_1 > 0, \ \ t \to \infty, \\
&\|\theta(t) - \theta^*\| \leq \frac{\varepsilon_1}{\omega_0} + \sqrt{\sum_{i=1}^{i=4} a_i^2 \sin(\omega_i t + \frac{\pi}{2})^2}, \\
&\quad \varepsilon_1 > 0, \ \ t \to \infty,
\end{aligned}$$

which finally implies, after using the fact that $\sin(\omega_i t + \frac{\pi}{2})^2 \leq 1$, and discretizing the time variable $t = \Delta T I$, $\|\theta(\Delta T k) - \theta^*\| \leq \frac{\varepsilon_1}{\omega_0} + \sqrt{\sum_{i=1}^{i=4} a_i^2}, k \to \infty$. □

Remark 2: Note that the upper-bound presented in Lemma 1, shows only existence of a small $\varepsilon_1 > 0$, s.t. the estimated error is bounded by a term proportional to ε_1, plus a term proportional to the dither signals amplitudes $a_i, i = 1, \cdots, 4$.

The important point here is that the term proportional to ε_1 is devided by the maximum of the extremum seeking dither signal's frequency $\omega_0 = max\{\omega_1, \cdots, \omega_4\}$. These frequencies have to be chosen large enough to make the term $\frac{\varepsilon_1}{\omega_0}$ negligeable compared to the remaining term $\sqrt{\sum_{i=1}^{i=4} a_i^2}$, which effectively bounds the estimation error by the choice of the dither signals amplitudes, which can then be tuned such that the estimation error is small, e.g., [33].

4. SOP ESTIMATION

To guarantee the safe and durable operation, the working current and voltage of the lithium-ion battery should be restricted in a range so that the battery power will be limited by the minimum value of the two restrictions given by

$$\begin{aligned}
SOP_{discharge} &= \min[\ SOP^V_{discharge} \quad SOP^I_{discharge}\ ], \\
SOP_{charge} &= \max[\ SOP^V_{charge} \quad SOP^I_{charge}\ ],
\end{aligned} \tag{13}$$

where $SOP_{discharge}$ and SOP_{charge} are the maximum discharging and charging capabilities of the battery, respectively, $SOP^V_{discharge}$ and SOP^V_{charge} are the battery SOPs under voltage limitation, $SOP^I_{discharge}$ and SOP^I_{charge} are the battery SOPs under current limitation.

4.1. SOP based on voltage limitation

In order to predict the maximum power capability under the voltage limitation, (9) is rewritten into

$$\begin{aligned}
\hat{SOC}(k+1) &= \hat{SOC}(k) - \frac{\eta T_s}{C_{max}} i_B(k), \\
\hat{V}_d(k+1) &= \gamma \hat{V}_d(k) + R_c(1-\gamma) i_B(k), \\
\hat{V}_h(k+1) &= H\hat{V}_h(k) + (H-1) sign(i_B(k)) V_{hmax}, \\
\hat{i}_B(k+1) &= [V_{oc}(\hat{SOC}(k+1)) - \hat{V}_d(k+1) \\
&\quad + \hat{V}_h(k+1) - V_B(k+1)]/R_s,
\end{aligned} \tag{14}$$

where the battery model parameters R_s, R_c, C_d, and C_{max} have been identified by the ES algorithm. The estimated current for the next time step $\hat{i}_B(k+1)$ can be obtained with a given $V_B(k+1)$.

According to (14), the maximum discharging and charging current can be obtained by setting $V_B(k+1)$ to the minimum and maximum limiting value. Then, the battery SOP can be obtained by multiplying the maximum discharging and charging current with the limiting voltage,

$$\begin{aligned}
SOP^V_{discharge}(k+1) &= V_{Bmin} \hat{i}_B(k+1)(V_{Bmin}), \\
SOP^V_{charge}(k+1) &= V_{Bmax} \hat{i}_B(k+1)(V_{Bmax}),
\end{aligned} \tag{15}$$

where $SOP^V_{discharge}(k+1)$ and $SOP^V_{charge}(k+1)$ are the maximum discharging and charging capabilities for the next sampling interval under the voltage limitation, V_{Bmax} and V_{Bmin} the maximum and minimum voltage allowed for the battery operation, respectively. With the updated $i_B(k)$ and $V_B(k)$, the algorithm above can periodically predict the SOP of the battery for the next time step.

4.2. SOP based on current limitation

The maximum charging and discharging currents of the battery are also limited and should be considered in the SOP estimation. In order to predict the maximum power capability under the current limitation, (9) is rewritten into

$$\begin{aligned}
\hat{SOC}(k+1) &= \hat{SOC}(k) - \frac{\eta T_s}{C_{max}} i_B(k), \\
\hat{V}_d(k+1) &= \gamma \hat{V}_d(k) + R_c(1-\gamma) i_B(k),
\end{aligned}$$

$$\hat{V}_h(k+1) = H\hat{V}_h(k) + (H-1)sign(i_B(k))V_{hmax},$$
$$\hat{V}_B(k+1) = V_{oc}(S\hat{O}C(k+1)) - \hat{V}_d(k+1) - R_s i_B(k+1) + \hat{V}_h(k+1), \quad (16)$$

where the battery model parameters R_s, R_c, C_d, and C_{max} have been identified by the ES algorithm. The estimated voltage for the next time step $\hat{V}_B(k+1)$ can be obtained with a given $i_B(k+1)$.

According to (16), by setting $i_B(k+1)$ to the minimum and maximum limiting value, $\hat{V}_B(k+1)$ can be calculated. Then, the battery SOP can be expressed as

$$SOP^I_{discharge}(k+1) = I_{Bmax}\hat{V}_B(k+1)(I_{Bmax}),$$
$$SOP^I_{charge}(k+1) = I_{Bmin}\hat{V}_B(k+1)(I_{Bmin}), \quad (17)$$

where $SOP^I_{discharge}(k+1)$ and $SOP^I_{charge}(k+1)$ are the maximum discharging and charging capabilities for the next sampling interval under the current limitation, I_{Bmax} and I_{Bmin} are the maximum discharging and charging currents allowed for the battery operation, respectively. With the updated $i_B(k)$ and $V_B(k)$, the algorithm above can periodically predict the SOP of the battery under the current limitation for the next time step.

5. SIMULATION RESULTS

Simulations are carried out in Matlab/Simulink to validate the proposed ES-based parameter identification method and the SOP prediction algorithm for a Li-ion battery. Two different types of current profile are applied to test the battery model: high pulse current cycle and the current profile based on real test data from standard UDDS.

5.1. High pulse current cycle

The battery model is first tested under a high pulse current cycle (i_B=10C, see Fig. 4(a)). This current profile leads to an output voltage profile shown in Fig. 4(b) from the battery model. Table 1 lists the values of the model parameters, which are based on a polymer Li-ion battery cell [28] with the maximum capacity scaled up to 10 Ah. The parameters used for the estimation algorithm in simulation are also listed in Table 1. The initial estimated states is $[SOC(0), V_d(0), V_h(0)]^T = [0.35, 0, 0]^T$. The initial values for the battery model parameters R_s, R_c, C_d, and

Table 1. Simulated battery model parameters.

C_{max}	$10Ah$	C_d	$4000F$	R_s	0.06Ω	R_c	0.02Ω
V_{hmax}	$0.01V$	ρ	$2.47e-4$	A_0	-0.852	A_1	63.867
A_2	3.692	A_3	0.559	A_4	0.51	A_5	0.508
a_1	0.005	a_2	0.01	a_3	170	a_4	0.9
ω_1	10	ω_2	80	ω_3	10	ω_4	10
l	1	K_p	100				

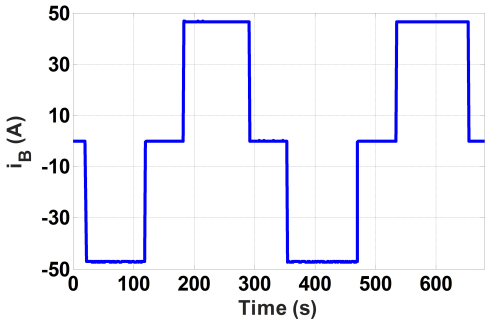

(a)

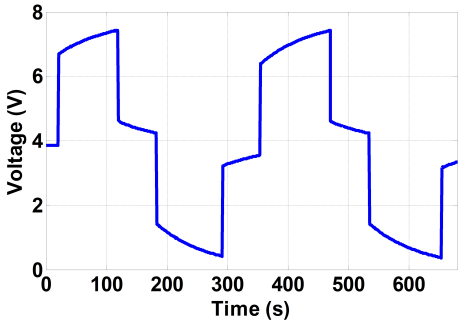

(b)

Fig. 4. High pulse current cycle: (a) input current profile, (b) cell voltage.

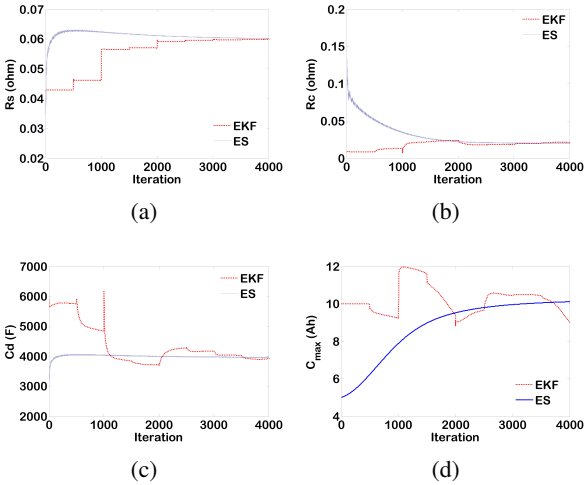

(a) (b) (c) (d)

Fig. 5. Simulation results of ES-based parameter identification for a Li-ion battery under high pulse current cycle: (a) estimated R_s, (b) estimated R_c, (c) estimated C_d, (d) estimated C_{max}.

C_{max} in the ES-based algorithm are 0.03, 0.06, 3000, and 5, respectively, the sampling time is 1 *sec*. Fig. 5 shows the results of the parameter identification by the proposed ES-based method and the basic EKF method. The identifi-

cation results are validated against the exact values of the battery parameters. The battery model parameters converge to their true values well after a certain number of iterations in the proposed method. Compared with the basic EKF method, the proposed method has a faster rate of convergence. Although R_s, R_c and C_d can converge to their true values, the process of convergence takes longer time, e.g., it needs about 3000 more iterations for C_d to converge. For parameter C_{max}, it does not converge to the true value after 4000 iteration. Fig. 6 shows the cost function during this process. The cost function decreases to a small value after the battery parameters converge, which indicates the estimated terminal voltage $\hat{V}_B$ from the battery model converges to the true value V_B.

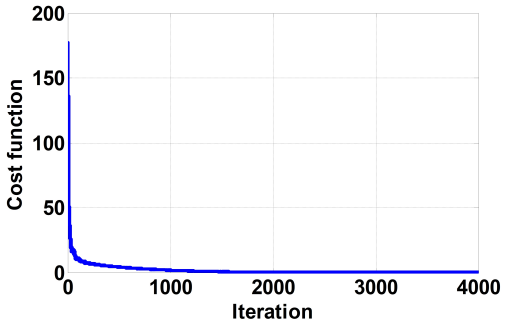

Fig. 6. Cost function under high pulse current cycle.

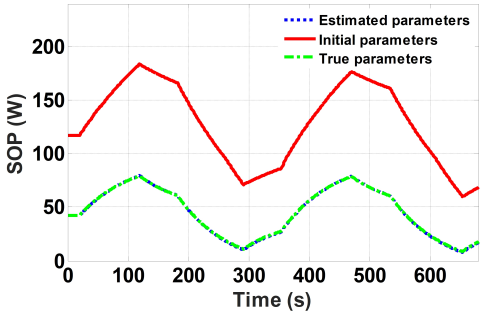

(a)

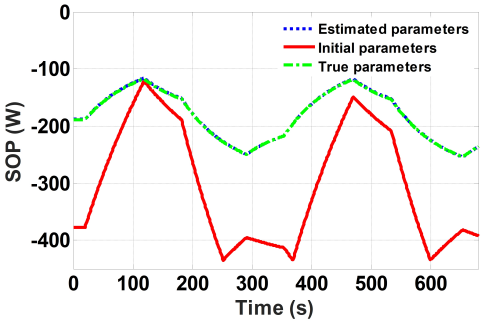

(b)

Fig. 7. SOP estimation: (a) for discharge, and (b) for charge.

Table 2. Performance of estimation algorithm for high pulse current cycle.

	R_s	R_c	C_d	C_{max}	$SOP_{discharge}$	SOP_{charge}
Estimation errors (%)	0.17	1.5	1.08	0.39	1.5	0.16
Computing time (s)	0.15	0.15	0.15	0.15	0.89	0.89

After the estimated battery parameters converge, their final values are used for the SOP prediction of the battery. Fig. 7 shows the results of the SOP prediction, in which positive power means discharging and negative power means charging. Three curves are provided in Fig. 7, which are the SOP prediction using the initial and final values of the battery model parameters, and the theoretical SOP respectively. It can be clearly observed that by using the estimated battery parameters obtained from the ES-based method, the predicted SOP overlaps with the theoretical SOP of the battery well. SOP prediction using the estimated parameters shows a high accuracy. Fig. 7 also shows that even a small divergence of the battery parameters will cause a large error of the predicted SOP, which indicates the importance of the battery parameter identification with high accuracy. Table 2 shows the performances of the parameter identification and SOP estimation algorithms. The battery parameters and SOP are estimated with high accuracy and short calculation time, as seen from Table 2.

5.2. Current profile in UDDS

The battery model is then subject to a current profile based on real test data from the standard UDDS. In an urban driving environment, a vehicle switches frequently between acceleration, deceleration and steady state, which would lead to battery discharging profiles containing sufficient frequencies, thus bringing about improved identifiability and observability of the battery model. This current profile is shown in Fig. 8(a), which leads to an output voltage profile shown in Fig. 8(b) from the battery model. The initial estimated states is $[SOC(0), V_d(0), V_h(0)]^T = [0.85, 0, 0]^T$. The initial values for the battery model parameters R_s, R_c, C_d, and C_{max} in the ES-based algorithm are 0.03, 0.06, 3000, and 5, respectively. Fig. 9 shows the results of the parameter identification by the proposed ES-based method and the basic EKF method. The battery model parameters converge to their true values well after a certain number of iterations in the proposed method. Again, the proposed method has a faster rate of convergence compared with the basic EKF method, e.g., it needs about 3000 more iterations for C_d to converge. For parameter C_{max}, it does not converge to the true value after 3000 iteration. Fig. 10 shows the cost function during this process. The cost function decreases to a small value af-

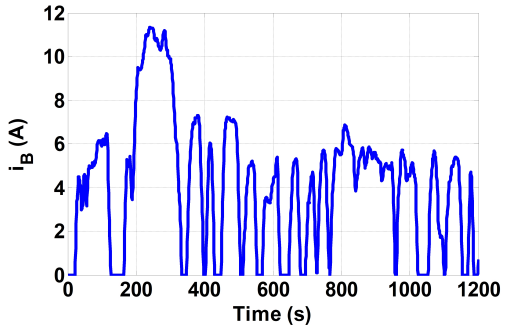

(a)

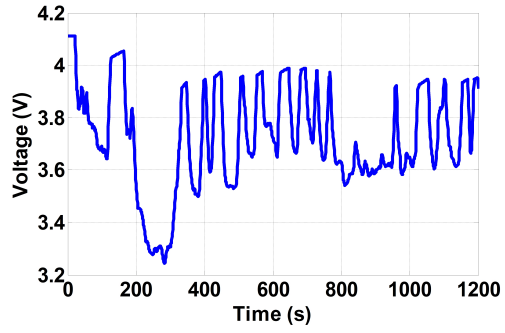

(b)

Fig. 8. UDDS current profile: (a) input current profile, (b) cell voltage.

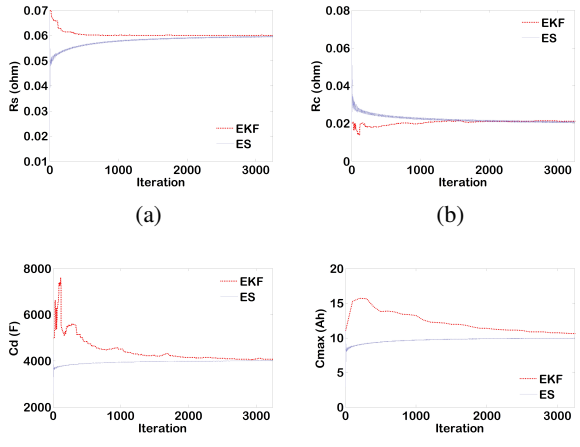

(a) (b) (c) (d)

Fig. 9. Simulation results of ES-based parameter identification for a Li-ion battery under UDDS current profile: (a) estimated R_s, (b) estimated R_c, (c) estimated C_d, (d) estimated C_{max}.

ter the battery parameters converge, which again indicates the estimated terminal voltage $\hat{V}_B$ from the battery model converges to the true value V_B.

After the estimated battery parameters converge, their final values are used for the SOP prediction of the battery. Fig. 11 shows the results of the SOP prediction. Three curves are provided in Fig. 11, which are the SOP prediction using the initial and final values of the battery model parameters, and theoretical SOP, respectively. It can be clearly observed that by using the estimated battery parameters obtained from the ES-based method, the predicted SOP overlaps with the theoretical SOP of the battery well. The proposed ES-based parameter identification method and the SOP prediction algorithm work well for the Li-ion battery under both the high pulse current cycle and the UDDS current profiles. Table 3 shows

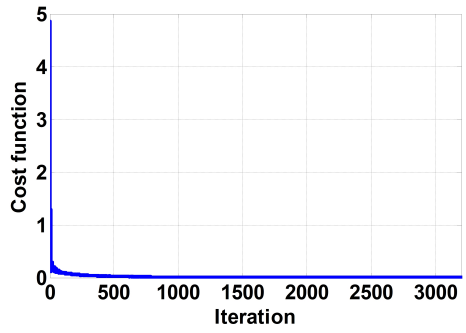

Fig. 10. Cost function under UDDS current cycle.

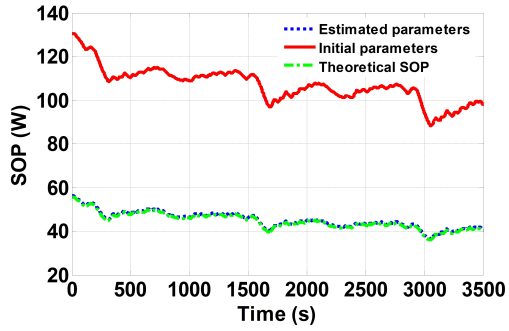

(a)

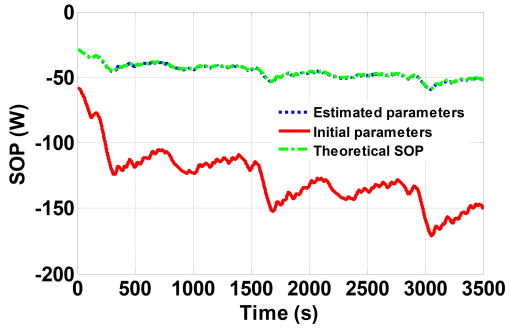

(b)

Fig. 11. SOP estimation: (a) for discharge, and (b) for charge.

Table 3. Performance of estimation algorithm for UDDS.

	R_s	R_c	C_d	C_{max}	$SOP_{discharge}$	SOP_{charge}
Estimation errors (%)	0.33	0.99	0.29	0.02	1.44	0.5
Computing time (s)	0.15	0.15	0.15	0.15	0.9	0.9

the performances of the parameter identification and SOP estimation algorithms. Again, the battery parameters and SOP are estimated with high accuracy and short calculation time, as seen from Table 3.

6. DISCUSSION

The ES algorithm itself is a model-free adaptive optimization method and has the advantages of both rigorously provable convergence and simple implementation, which enables it to be used in the real system. Compared with the EKF method, ES can identify multiple battery parameters with faster convergence, higher accuracy, and simpler implementation, as shown in Fig. 5 and Fig. 9. In order to achieve a successful parameter estimation of the proposed ES method, the cost function and the parameters should be selected properly. For the cost function, the error of the system output, such as voltage in (10), can be used and a larger K_p can lead to a faster convergence. For the algorithm parameters, the frequency ω_i should be large enough to ensure the convergence of ES, and the selection of a_i relates to the true parameter value. For large parameters, larger values of a_i are usually chosen.

The SOP can be easily obtained from the battery model incorporated with the battery open-circuit voltage, after the parameter estimation by the ES. The simplicity and accuracy of the ES increase the accuracy of SOP prediction. Compared with previous SOP estimation algorithms that only consider the voltage limitation, the estimation method in this paper considers both the voltage and current limitations of the battery, which provides a two-level estimation of the battery peak power capabilities. This contributes to fully exploit the potential of the battery within the safe operation range.

Recently, a new control algorithm named composite learning from adaptive dynamic surface control was proposed in [31]. The composite learning was proposed to update parametric estimates for systems with mismatched parametric uncertainties. It will be a good choice to extend the composite learning technique to the battery systems for online parameter estimation for future work, as the battery systems especially in electric vehicles are highly nonlinear with uncertainties.

7. CONCLUSION

In this paper we have proposed a novel parameter identification method and its application to SOP prediction for lithium-ion batteries. The ES algorithm has been developed for identifying the parameters of batteries on the basis of an electrical circuit model incorporating hysteresis effect. A rigorous convergence proof of the ES-based estimation algorithm is provided. Based on the electrical circuit model with the identified parameters, a battery SOP prediction algorithm has been developed, which considers both the voltage and current limitations of the battery. Simulation results for lithium-ion batteries have been provided to validate the proposed parameter identification and SOP prediction methods, for both high impulse and UDDS current profiles. The proposed method is suitable for real operation of embedded BMS due to its low complexity and numerical stability. Future research will focus on the development of advanced algorithms for comprehensive battery state estimation such as SOC, SOP, and SOH, and fault diagnosis, prognosis, and optimization of battery management systems.

REFERENCES

[1] V. Minh and J. Pumwa, "Simulation and control of hybrid electric vehicles," *International Journal of Control, Automation and Systems*, vol. 10, no. 2, pp. 308-316, April 2012.

[2] S. Han, H. Aki, S. Han, B. Kwon, and J. Park, "Optimal charging strategy for a residential PEV battery considering bidirectional trade and frequency regulation," *International Journal of Control, Automation and Systems*, vol. 14, no. 2, pp. 587-597, April 2016.

[3] J. Cao and B. Cao, "Neural network sliding mode control based on on-line identification for electric vehicle with ultracapacitor-battery hybrid power," *International Journal of Control, Automation and Systems*, vol. 7, no. 3, pp. 409-418, June 2009.

[4] R. Wongsathan and A. Nuangnit, "Optimal hybrid neuro-fuzzy based controller using MOGA for photovoltaic (PV) battery charging system," *International Journal of Control, Automation and Systems*, vol. 16, no. 6, pp. 3036-3046, December 2018.

[5] G. Plett, "Extended Kalman filtering for battery management systems of LiPB-based HEV battery packs - Part 3. State and parameter estimation," *J. Power Sources*, vol. 134, no. 2, pp. 262-276, August 2004.

[6] G. Plett, "Sigma-point Kalman filtering for battery management systems of LiPB-based HEV battery packs: Part 2. Simultaneous state and parameter estimation," *J. Power Sources*, vol. 161, no. 2, pp. 1369-1384, October 2006.

[7] Z. Chen, Y. Fu, and C. Mi, "State of charge estimation of lithium-ion batteries in electric drive vehicles using extended Kalman filtering," *IEEE Trans. Vehicular Technology*, vol. 62, no. 3, pp. 1020-1030, March 2013.

[8] J. D. Rubio, "Stable Kalman filter and neural network for the chaotic systems identification," *Journal of the Franklin Institute*, vol. 354, no. 16, pp. 7444-7462, November 2017.

[9] E. Lughofer, S. Kindermann, M. Pratama, and J. D. Rubio, "Top-down sparse fuzzy regression modeling from data with improved coverage," *International Journal of Fuzzy Systems*, vol. 19, no. 5, pp. 1645-1658, October 2017.

[10] J. D. Rubio, E. Lughofer, J. A. Meda-Campana, L. A. Paramo, J. F. Novoa, and J. Pacheco, "Neural network updating via argument Kalman filter for modeling of Takagi-Sugeno fuzzy models," *Journal of Intelligent & Fuzzy Systems*, vol. 35, no. 2, pp. 2585-2596, 2018.

[11] J. D. Rubio, E. Lughofer, P. Angelov, and J. Novoa, "A novel algorithm for the modeling of complex processes," *Kybernetika*, vol. 54, no. 1, pp. 79-95, 2018.

[12] G. Giordano, V. Klass, M. Behm, G. Lindbergh, and J. Sjoberg, "Model-based lithium-ion battery resistance estimation from electric vehicle operating data," *IEEE Trans. Vehicular Technology*, vol. 67, no. 5, pp. 3720-3728, May 2018.

[13] M. Roscher, O. Bohlen, and D. Sauer, "Reliable state estimation of multicell lithium-ion battery system," *IEEE Trans. Energy Conv.*, vol. 26, no. 3, pp. 737-743, September 2011.

[14] C. Gould, C. Bingham, D. Stone, and P. Bentley, "New battery model and state-of-health determination through subspace parameter estimation and state-observer techniques," *IEEE Trans. Vehicular Technology*, vol. 58, no. 8, pp. 3905-3916, October 2009.

[15] A. Fotouhi, D. Auger, K. Propp, and S. Longo, "Electric vehicle battery parameter identification and SOC observability analysis: NiMH and Li-S case studies," *IET Power Electron.*, vol. 10, no. 11, pp. 1289-1297, September 2017.

[16] X. Chen, W. Shen, M. Dai, Z. Cao, J. Jin, and A. Kapoor, "Robust adaptive sliding-mode observer using RBF neural network for lithium-ion battery state of charge estimation in electric vehicle," *IEEE Trans. Vehicular Technology*, vol. 65, no. 4, pp. 1936-1947, April 2016.

[17] Y. Zhang, C. Zhang, and X. Zhang, "State-of-charge estimation of the lithium-ion battery system with time-varying parameter for hybrid electric vehicles," *IET Control Theory Appl.*, vol. 8, no. 3, pp. 160-167, Feburary 2014.

[18] W. Shen and H. Li, "A sensitivity-based group-wise parameter identification algorithm for the electric model of li-ion battery," *IEEE Access*, vol. 8, pp. 4377-4387, March 2017.

[19] T. Feng, L. Yang, X. Zhao, H. Zhang, and J. Qiang, "Online identification of lithium-ion battery parameters based on an improved equivalent-circuit model and its implementation on battery state-of-power prediction," *J. Power Sources*, vol. 281, pp. 192-203, May 2015.

[20] F. Sun, R. Xiong, H. He, W. Li, and J. Aussems, "Model-based dynamic multi-parameter method for peak power estimation of lithium-ion batteries," *Applied Energy*, vol. 96, pp. 378-386, August 2012.

[21] R. Xiong, H. He, F. Sun, X. Liu, and Z. Liu, "Model-based state-of-charge and peak power capability joint estimation for lithium-ion battery in plug-in hybrid electric vehicles," *J. Power Sources*, vol. 229, pp. 159-169, May 2013.

[22] P. Malysz, J. Ye, R. Gu, H. Yang, and A. Emadi, "Battery state-of-power peak current calculation and verification using an asymmetric parameter equivalent circuit model," *IEEE Trans. Vehicular Technology*, vol. 65, no. 6, pp. 4512-4522, June 2016.

[23] J. Lu, Z. Chen, Y. Yang, and M. Lv, "Online estimation of state of power for lithium-ion batteries in electric vehicles using genetic algorithm," *IEEE Access*, vol. 6, pp. 20868-20880, April 2018.

[24] M. Benosman and G. Atinc, "Multi-parametric extremum seeking-based learning control for electromagnetic actuators," *International Journal of Control*, vol. 88, no. 3, pp. 517-530, April 2015.

[25] M. Benosman, *Learning-based Adaptive Control: An Extremum Seeking Approach, Theory and Applications*, Elsevier, July 2016.

[26] M. Krstic, "Performance improvement and limitations in extremum seeking control," *Systems & Control Letters*, vol. 39, pp. 313-326, April 2000.

[27] M. Rotea, "Analysis of multivariable extremum seeking algorithms," *Proc. American Control Conf.*, Chicago, USA, pp. 433-437, June 2000.

[28] T. Kim and W. Qiao, "A hybrid battery model capable of capturing dynamic circuit characteristics and nonlinear capacity effects," *IEEE Trans. Energy Conv.*, vol. 26, no. 4, pp. 1172-1180, December 2011.

[29] M. Verbrugge and E. Tate, "Adaptive state of charge algorithm for nickel metal hydride batteries including hysteresis phenomena," *J. Power Sources*, vol. 126, pp. 236-249, Feburary 2004.

[30] T. Kim, Y. Wang, H. Fang, Z. Sahinoglu, and T. Wada, "Model-based condition monitoring for lithium-ion batteries," *J. Power Sources*, vol. 295, pp. 16-27, November 2015.

[31] Y. Pan and H. Yu, "Composite learning from adaptive dynamic surface control," *IEEE Trans. Automatic Control*, vol. 61, no. 9, pp. 2603-2609, September 2016.

[32] M. Benosman, "Multi-parametric extremum seeking-based auto-tuning for robust input-output linearization control," *International Journal of Robust and Nonlinear Control*, vol. 26, no. 18, pp. 4035-4055, 2016.

[33] Y. Tan, D .Nesic, and I. Mareels, "On the choice of dither in extremum seeking systems: a case study," *Automatica*, vol. 44, no. 5, pp. 1446-1450, May 2008.

Chun Wei received his B.S. degree in electrical engineering from Beijing Jiaotong University, Beijing, China, in 2009, an M.S. degree in electrical engineering from North China Electric Power University, Beijing, China, in 2012, and a Ph.D. degree in electrical engineering from the University of Nebraska-Lincoln, Lincoln, NE, USA, in 2016. He was a postdoctoral researcher in ABB Corporate Research Center, Raleigh, NC, USA in year 2017. He is currently an Associate Professor with College of Information Engineering, Zhejiang University of Technology, Hangzhou, Zhejiang, China. His research interests include renewable energy generation systems, adaptive control, motor drives, and system identification.

Mouhacine Benosman is a Senior Research Scientist at Mitsubishi Electric Research Labs (MERL) in Cambridge, USA. Before joining MERL, he worked at Reims University, France, Strathclyde University, Scotland, and National University of Singapore. His research interests include modeling and control of flexible systems, nonlinear robust and fault tolerant control, multi-agent distributed control with applications to robotics and smart-grid systems, and learning and adaptive control for nonlinear systems. Mouhacine has published a monograph about learning-based adaptive control, more than 100 peer-reviewed journal articles and conference papers, and more than 20 patents in the field of mechatronics systems control. He is a senior member of the IEEE, Associate Editor of the Control System Society Conference Editorial Board, Associate Editor of the Journal of Optimization Theory and Applications, and Senior Editor of the International Journal of Adaptive Control and Signal Processing.

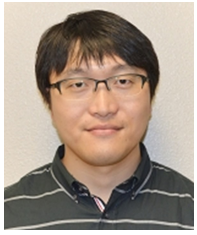

Taesic Kim received his M.S. degree in Electrical Engineering and his Ph.D. degree in Computer Engineering at the University of Nebraska-Lincoln, in 2012 and 2015, respectively. In 2009, He was with the New and Renewable Energy Research Group of Korea Electrotechnology Research Institute, Korea. He was also with Mitsubishi Electric Research Laboratories, Cambridge, MA, USA in 2013. Currently, He is an assistant professor in the Department of Electrical Engineering and Computer Science at the Texas A&M University-Kingsville. He research focuses on energy IoT, power electronics, cyber and physical security, blockchain, and intelligence algorithms for power and energy systems. He holds 2 U.S. patents and co-authored more than 40 papers in refereed journals and IEEE conference proceedings in the field of cyber-physical power and energy systems. He is a Cyber Physical Security Steering Committee for IEEE PELS and a Guest Associate Editor of the IEEE Journal of Emerging and Selective Topics in Power Electronics.